



Features of MOG required for recognition by patients with MOG antibody-associated disorders

Caterina Macrini,¹ Ramona Gerhards,¹ Stephan Winklmeier,¹ Lena Bergmann,² Simone Mader,¹ Melania Spadaro,¹ Atay Vural,³  Michaela Smolle,^{2,4} Reinhard Hohlfeld,¹ Tania Kümpfel,¹ Stefan F. Lichtenthaler,^{5,6} Henri G. Franquelim,⁷ Dieter Jenne⁸ and  Edgar Meinl¹

Antibodies to myelin oligodendrocyte glycoprotein (MOG-Abs) define a distinct disease entity. Here we aimed to understand essential structural features of MOG required for recognition by autoantibodies from patients. We produced the N-terminal part of MOG in a conformationally correct form; this domain was insufficient to identify patients with MOG-Abs by ELISA even after site-directed binding. This was neither due to a lack of lipid embedding nor to a missing putative epitope at the C-terminus, which we confirmed to be an intracellular domain. When MOG was displayed on transfected cells, patients with MOG-Abs recognized full-length MOG much better than its N-terminal part with the first hydrophobic domain ($P < 0.0001$). Even antibodies affinity-purified with the extracellular part of MOG recognized full-length MOG better than the extracellular part of MOG after transfection. The second hydrophobic domain of MOG enhanced the recognition of the extracellular part of MOG by antibodies from patients as seen with truncated variants of MOG.

We confirmed the pivotal role of the second hydrophobic domain by fusing the intracellular part of MOG from the evolutionary distant opossum to the human extracellular part; the chimeric construct restored the antibody binding completely. Further, we found that in contrast to 8-18C5, MOG-Abs from patients bound preferentially as $F(ab)_2$ rather than Fab. It was previously found that bivalent binding of human IgG1, the prominent isotype of MOG-Abs, requires that its target antigen is displayed at a distance of 13–16 nm. We found that, upon transfection, molecules of MOG did not interact so closely to induce a Förster resonance energy transfer signal, indicating that they are more than 6 nm apart.

We propose that the intracellular part of MOG holds the monomers apart at a suitable distance for bivalent binding; this could explain why a cell-based assay is needed to identify MOG-Abs. Our finding that MOG-Abs from most patients require bivalent binding has implications for understanding the pathogenesis of MOG-Ab associated disorders. Since bivalently bound antibodies have been reported to only poorly bind C1q, we speculate that the pathogenicity of MOG-Abs is mostly mediated by other mechanisms than complement activation. Therefore, therapeutic inhibition of complement activation should be less efficient in MOG-Ab associated disorders than in patients with antibodies to aquaporin-4.

- 1 Institute of Clinical Neuroimmunology, Biomedical Center and University Hospitals, Ludwig-Maximilians-Universität München, 82152 Munich, Germany
- 2 Physiological Chemistry, Biomedical Center, Ludwig-Maximilians-Universität, 82152 Munich, Germany
- 3 Department of Neurology, Koc University School of Medicine, 34450 Istanbul, Turkey
- 4 BioPhysics Core Facility, Biomedical Center, Ludwig-Maximilians-Universität, 82152 Munich, Germany

Received August 13, 2020. Revised December 21, 2020. Accepted January 08, 2021. Advance access publication March 11, 2021

© The Author(s) (2021). Published by Oxford University Press on behalf of the Guarantors of Brain. All rights reserved.

For permissions, please email: journals.permissions@oup.com

- 5 German Center for Neurodegenerative Diseases (DZNE) Munich and Neuroproteomics, School of Medicine, Klinikum rechts der Isar, Technical University of Munich, 81675 Munich, Germany
 6 Munich Cluster for Systems Neurology (SyNergy), 81377 Munich, Germany
 7 Cellular and Molecular Biophysics, Max Planck Institute of Biochemistry, 82152 Munich, Germany
 8 Institute of Lung Biology and Disease (ILBD), Comprehensive Pneumology Center (CPC), 81377 Munich, Germany

Correspondence to: Dr Edgar Meinl
 Institute of Clinical Neuroimmunology, Biomedical Center and University Hospitals
 Ludwig-Maximilians-Universität München
 Großhaderner Str. 9, 82152 Planegg-Martinsried, Germany
 E-mail: Edgar.Meinl@med.uni-muenchen.de

Keywords: autoimmunity; antigen-recognition; demyelination; neuroinflammation to MOG

Abbreviations: Abs = antibodies; CBA = cell-based assay; ECFP = enhanced cyan fluorescent protein; EGFP = enhanced green fluorescent protein; EYFP = enhanced yellow fluorescent protein; FRET = Förster resonance energy transfer; mAb = monoclonal antibody

Introduction

The identification of autoantibodies (Abs) in patients with inflammatory diseases of the CNS helps to establish a specific diagnosis, which is critical for understanding the pathogenesis and for therapy optimization.^{1,2} The recognition of autoantibodies may eventually result in the definition of separate diseases. For example, consensus is now emerging that autoantibodies to myelin oligodendrocyte glycoprotein (MOG) define a separate disease entity, MOG antibody-associated disorders (MOGAD).^{3–9}

MOG is displayed on the outer surface of internodal myelin and, due to this position, it is a target of pathogenic antibodies. While it has been demonstrated since the 1980s that autoantibodies to MOG induce demyelination in rodent and primate models of multiple sclerosis,^{10,11} the unequivocal identification of MOG-Abs in the blood of patients was achieved much later.¹² MOG-Abs were subsequently connected to acquired demyelinating diseases in children^{13–15} and later also to adults with inflammation in the CNS (reviewed in Reindl and Waters⁶).

One reason for the difficulty in identifying patients with MOG-Abs initially was the fundamental difference of MOG-Abs obtained in animal models and MOG-Abs in patients. In animal models, MOG-Abs were readily detected by ELISA,^{16,17} whereas pathogenic monoclonal antibodies (mAbs) from animals recognized MOG both by ELISA and on the surface of transfected cells.¹⁸ To identify patients with MOG-Abs, there is now consensus that an assay using cells transfected with full-length MOG is needed.^{19,20}

MOG is displayed on the membrane. The structure of its extracellular N-terminal part was determined by X-ray crystallography; it forms an Ig-V fold consisting of two antiparallel β -sheets.^{21,22} The prototype rodent anti-MOG mAb 8-18C5 binds to three loops linking the β -sheets of this N-terminal part with a dominant contribution of His103 and Ser104 in the centre of the FG loop.^{21,23} MOG-Abs derived from patients are heterogeneous and bind to different loops linking the β -sheets.^{19,24,25} This N-terminal part of MOG has been recombinantly produced in its correctly folded form and was used for affinity purification of selected patients' antibodies²⁶ as well as detection of MOG-Abs in a few patients.¹⁹ Thus, the precise conformation of MOG is essential to identify patients with MOG-Abs and correctly folded N-terminal part of MOG alone is not sufficient. The reason for this is currently unknown.

While there is consensus on the extracellular localization and structure of the N-terminal part of MOG, there is dissent about the localization of its C-terminus. Earlier papers indicated that the

C-terminus is intracellular,^{27,28} whereas currently UniProt (27 November 2020) and a recent detailed review with reference to UniProt²⁹ presented a model where the C-terminus of MOG was localized extracellularly. Thus, it is unclear if this part of MOG contributes to antigen recognition in patients.

The aim of our study was to gain further insights into details of antigen recognition by MOG-Abs from patients. Specifically, we wanted to understand why a cell-based assay (CBA) is needed to identify patients with MOG-Abs and why the N-terminal external domain of MOG in the correct conformation is not sufficient. To investigate this, we produced the N-terminal part of MOG recombinantly in a correctly folded way and bound it in a site-directed manner to a solid-phase or to lipid-coated beads, then analysed the recognition by MOG-Abs. We revisited the localization of the C-terminal part of MOG with an antibody specific for the C-terminus. We analysed in detail 14 patients with MOG-Abs using truncated variants of MOG and domain-swapping with parts of the evolutionary distant opossum. We prepared Fab and F(ab')₂ fragments to analyse monovalent versus bivalent binding and used Förster resonance energy transfer (FRET) to analyse whether MOG monomers interacted closely with each other.

Our different experimental approaches revealed that most MOG-Abs from patients, but not the prototypic rodent mAb 8-18C5, require the intramembrane second hydrophobic domain for MOG recognition and bivalent binding is needed. We propose a model in which the second hydrophobic domain of MOG makes two kinks in the membrane around two conserved prolines and is localized within the inner cytosolic membrane leaflet, in agreement with previous reports.^{27,28} This structural feature would thereby facilitate lateral clustering and spacing of the extracellular N-terminal part of MOG that allows bivalent binding of autoantibodies. This could explain why a CBA with full-length MOG is needed to identify patients with MOG-Abs. Importantly, the bivalent binding of MOG-Abs has implications for our concepts of pathogenicity of MOG-Abs and therapeutic strategies.

Materials and methods

MOG variants

Constructs coding for the different variants of the intracellular part of MOG were synthesized from GeneArt (Thermo Fisher Scientific) and then cloned into the pEGFP-N1 vector (Clontech Laboratories) fusing the C-terminus to an enhanced green

fluorescent protein (EGFP) tag. The ED-MOG (1–155) construct was truncated at glycine-155, thus comprising the whole external domain, the first hydrophobic domain and part of the cytosolic domain.³⁰ The whole intracellular cytosolic portion was included in construct MOG-Cyt by ending the protein at the tyrosine-181. MOG-2TMD includes the whole second hydrophobic domain (to leucine-202) of full-length MOG (FL-MOG). The native C-terminus of this construct was substituted with a SGSGGGSGGGSGS linker. The numbering of these constructs is according to Breithaupt *et al.*²¹ and Mayer *et al.*²⁵ beginning with the first coding amino acids (GQF . . .) and not with the signal peptide.

The MOG sequence of opossum (*Monodelphis domestica*) was taken from the NCBI database and then ordered from Thermo Fisher Scientific GeneArt service. The chimeric construct, named Human-Opossum MOG, was designed with human MOG sequence until glycine-155 followed by the cytosolic and second hydrophobic domain from the MOG sequence of the opossum. In this construct, the C-terminus consists of an SGSGGGSGGGSGS linker. Schemes of these constructs are included in Fig. 4. Mutants of the N-terminal extracellular part of MOG were described previously.²⁵

The MOG variants EYFP/CFP-FL-MOG and EYFP/CFP-ED-MOG, with the fluorescent dyes at the N-terminus were also synthesized from GeneArt (Thermo Fisher Scientific) and then cloned into the pEGFP-N1 vector, with the consequent removal of the EGFP sequence portion at the C-terminus. The control constructs enhanced cyan fluorescent protein (ECFP), enhanced yellow fluorescent protein (EYFP) and the fusion ECFP-EYFP were kindly provided by H. Eibel (Freiburg, Germany) and are described in Smulski *et al.*³¹

Lipids

The lipids are as follows: 1,2-dioleoyl-*sn*-glycero-3-phosphocholine (dioleoylphosphatidylcholine; DOPC) (Avanti Polar Lipids); 1,2-dioleoyl-*sn*-glycero-3-phosphoethanolamine-*N*-(cap biotinyl) (18:1 Biotinyl Cap PE) (Avanti Polar Lipids); and 1,2-dioleoyl-*sn*-glycero-3-phosphoethanolamine labelled with Atto 488 (Atto488 DOPE) (Sigma Aldrich).

Recombinant production of the correctly folded extracellular part of MOG

The extracellular part of human MOG (amino acids 1–125) with an Avi-tag allowing enzymatic biotinylation and a His-tag was recombinantly produced using the HEK-EBNA cells and the pTT5 vector.³² MOG-1–125 was secreted in serum-free supernatant, purified via its His-tag and its correct folding was assessed using circular dichroism, as described.^{24,26} The glycan of this MOG-1–125 has a similar size as the glycan of FL-MOG on transfected cells and its glycoforms have been described.²⁴ This material was used for ELISA, for binding to lipid-coated beads and for affinity-purification of MOG-Abs.

Affinity purification of MOG-Abs from patients

The autoantibodies against MOG present in the plasma of Patient 7 were affinity purified using the correctly folded extracellular part of MOG bound to streptavidin columns, as previously described.²⁶

ELISAs detecting MOG-Abs and recombinant monoclonal antibodies

We applied two ELISAs. First, MOG-1–125 was bound to MaxiSorp™ (Thermo Fisher Scientific) and compared with bovine serum albumin (BSA)-coated wells. Second, MOG-1–125 was biotinylated at its Avi-tag with the BirA biotin ligase Kit (Avidity) and

then bound to streptavidin plates and compared to streptavidin wells, since we saw that adding BSA to streptavidin-coated plates resulted in essentially the same results as using streptavidin-coated plates alone. The ELISA assays were validated using a recombinant mAb against MOG (r8-18C5) and a control mAb against Borrelia (HK-3) (Supplementary Fig. 1), both having a human IgG1-Fc part.^{26,33} Serum was diluted 1:200 and binding of antibodies was detected with an anti-human IgG conjugated to horseradish peroxidase (Jackson ImmunoResearch).

Localization of the C-terminus of MOG

Two different cell lines were used for this part of our study: HeLa cells transiently transfected with FL-MOG or ED-MOG, each fused to EYFP at the N-terminus and the TE-671 cell line (rhabdomyosarcoma cells) stably transfected with FL-MOG without any fluorescent tag.¹⁵ HeLa cells were fixed with 2% paraformaldehyde and permeabilized with Intracellular Staining Permeabilization Wash Buffer (BioLegend). TE671 cells were fixed and permeabilized with Cyto-Fast™ Fix/Perm Buffer Set (BioLegend). To detect MOG, the r8-18C5 antibody, which binds to the FG-loop in the extracellular part of MOG²¹ and the commercially available Ab28766 antibody (Abcam), which binds the last 12 amino acids of MOG at the C-terminus (AGQFLEELRNPF), were applied.

Lipid coating of silica beads and binding of MOG

Silica beads (SiO₂-R-6.0) of 6.16 μm in diameter (microParticles) were coated with a lipid bilayer as follows. First, a mixture of DOPC, Biotinyl CAP PE, Atto488 DOPE in chloroform was prepared at a 98:1:0.03 molar ratio inside a glass vial. A lipid film was formed on the walls of the vial by gently evaporating the solvent with a nitrogen stream and by subsequently drying under vacuum for 20 min. The lipid film was then rehydrated with 200 μl of PBS (Gibco, Thermo Scientific), 100 μl beads solution (at 6 mg/ml of concentration) and resuspended by vortexing until the solution became turbid. Following this, the beads were coated with the lipids through 30 min of sonication in a bath sonicator until the solution cleared.

The extent of the coating was determined in the first place by checking the green fluorescent signal of Atto488 DOPE on the beads via confocal microscopy imaging with an LSM 780 microscope using a 40×/1.2 W C-Apochromat objective (Carl Zeiss AG). We bound the biotinylated MOG-1–125 with neutravidin (Invitrogen) to the biotinyl CAP PE. We showed that it was displayed on the coated beads surface by detecting it with the r8-18C5 and Alexa Fluor® 647 goat anti-human IgG (H + L) antibody (Invitrogen) as the secondary antibody. The fluorescent signal was detected by confocal microscope imaging and by flow cytometry with FACSverse (BD Biosciences).

Quantification of anti-MOG reactivity on lipid-coated beads

We quantified the anti-MOG reactivity of several sera and of the humanized r8-18C5 by flow cytometry (BD Biosciences). We gated all the fluorescent beads with an Atto488 signal > 100 and then calculated their mean fluorescence intensity (MFI) in the APC channel. The MFI ratio was obtained by dividing the MFI of the beads bound to biotinylated MOG-1–125 incubated with sera or r8-18C5 by the MFI of the fluorescent beads not bound by biotinylated-MOG-1–125 incubated with sera or r8-18C5. All signals were quantified using FlowJo software (LLC, BD life sciences).

To test for recognition by sera with MOG-Abs, the beads were resuspended in 400 μl of FACS buffer, and 100 μl was then

incubated with serum diluted 1:50 in FACS buffer. Binding of antibodies in serum was detected with Alexa Fluor® 647 goat anti-human IgG (H + L) antibody (Invitrogen). The fluorescent signal was detected by flow cytometry with FACSverse (BD Biosciences).

Cell-based assay to quantify recognition of MOG variants

The reactivity of the patients' antibody to the different MOG variants was detected in a live CBA, as previously described^{25,26} with a FACSverse flowcytometer (BD Biosciences). HeLa cells were transiently transfected via Lipofectamine® 2000 (Thermo Fisher Scientific) with the different MOG constructs or with EGFP alone (control). To detect the binding of antibodies in serum (diluted 1:50) to the transfected cells, we used biotin-SP-conjugated goat anti-human IgG (1:500 diluted) (Jackson ImmunoResearch) as secondary antibody. Subsequently, Alexa Fluor® 647-conjugated streptavidin was added (1:2000). Dead cells were excluded from the experiment with propidium iodide staining (1:2000 in PBS).

All of our MOG constructs were expressed as fusion proteins with EGFP allowing the direct quantification of MOG expression via the EGFP signal. We noted that the different MOG constructs were expressed to a different intensity (Supplementary Fig. 2). This was taken into consideration and the gating for the default quantification was set to EGFP 100–500, because all MOG constructs showed a decent expression with these gating criteria (Supplementary Fig. 2A). Thus, the anti-MOG reactivity was quantified by gating the cells with EGFP signal between 100 and 500 and determining their MFI in the APC channel. We subsequently calculated the MFI ratio of cells expressing MOG-EGFP and cells expressing EGFP alone. All signals were quantified using Flowjo software (LLC, BD life sciences, Ashland, OR, USA).

Consideration of different expression intensities of the applied MOG mutants

We displayed all MOG variants as EGFP-fusion proteins as this allowed a precise quantification of MOG expression. We noted that the six MOG mutants differed in their intensity of expression. MOG-2TMD and human opossum-MOG showed the highest expression (Supplementary Fig. 2). All MOG constructs yielded a decent expression within the EGFP gate of 100–500 (Supplementary Fig. 2). Therefore, this EGFP gate of 100–500 was our default setting for quantification of the reactivity towards the different constructs.

We show the reactivity towards each MOG construct for all analysed patients using two different gateings, EGFP > 100 and EGFP 100–500 (Supplementary Fig. 3A and B). While in most instances the graphs in Supplementary Fig. 3A and B look similar, these two presentations provide complementary information in special instances. For example, for Patient 22 the response to ED-MOG appears higher than FL-MOG in Supplementary Fig. 3B, but when considering the EGFP gates of 100–500, it becomes clear that this patient similarly recognized ED-MOG and FL-MOG. Thus, the apparently higher response to ED-MOG of Patient 22 was only due to the higher percentage of cells expressing higher levels of ED-MOG than FL-MOG. This also applies to Patients 14, 38, 41, 42 and 16, whose reactivity to ED-MOG would be missed completely with the gate setting of EGFP 100–500.

Förster resonance energy transfer experiment to assess MOG dimerization

We carried out our FRET experiments as previously described.³¹ In brief, we transiently transfected HEK293T cells with the ECFP and EYFP-MOG fusion constructs. The cells were subsequently analysed 16–20 h post-transfection. All FRET experiments were performed

with a LSR Fortessa (BD Biosciences). The EYFP signal was detected using the 488 nm laser with a 540/30 filter, ECFP signal was detected using the 405 nm laser with a 450/40 filter and FRET signal was recorded using the 405 nm laser with a 540/30 filter. We defined the positive FRET gating by using cells expressing an ECFP–EYFP fusion protein as positive control. To define the FRET negative gating, cells were co-transfected with ECFP and EYFP.

Production of Fab and F(ab')₂ from patient plasma and analysis of their MOG recognition

IgG was purified from plasma with Protein G HP SpinTrap columns (GE Healthcare Life Sciences). Subsequently, the IgG concentration was measured with a Human IgG ELISA kit (Mabtech). The IgG concentration range of the purified plasma samples spanned between 2.5 and 7 mg/ml. Fab and F(ab')₂ fragments were then generated with the Pierce Fab/F(ab')₂ Preparation Kit (Thermo Fisher Scientific). The Fab fragments were further purified by size exclusion chromatography to separate them from the pool of undigested IgGs using a Superdex™ 200 Increase 10/300 GL column (GE Healthcare Life Sciences). Peak fractions were analysed by SDS-PAGE and Coomassie staining, elution fractions containing only digested Fabs were finally pooled and used for downstream assays.

To detect binding of the Fab and F(ab')₂ fragments to MOG, a different secondary antibody from the one used for detection of anti-MOG in serum had to be used, since the secondary antibody used for evaluating serum includes reactivity to the Fc-part of the IgG, which is no longer present after the Fab and F(ab')₂ preparation. We used an Alexa Fluor® 647 mouse anti-human Ig light chain κ antibody together with an Alexa Fluor® 647 mouse anti-human Ig light chain λ antibody, both 1:100 diluted (BioLegend). The fluorescent signal was further amplified by the use of a rat anti-mouse IgG Alexa Fluor® 647 antibody diluted 1:500 (Jackson ImmunoResearch). The r8-18C5 antibody was produced recombinantly with the human heavy chain from the J-element onwards, but a murine light chain.^{26,33} Therefore, this antibody and its Fab and F(ab')₂ were detected with an anti-human IgG + IgA + IgM (H + L) (Jackson ImmunoResearch) as secondary antibody.

Statistics

For statistical analysis, we used GraphPad Prism7 (GraphPad software, San Diego, CA, USA). For the quantification of the reactivity of the 14 patients with MOG-Abs towards the six different MOG variants we set the reactivity towards FL-MOG to 100% and normalized the reactivity towards the other constructs. We then used a one-way ANOVA Tukey's multiple test comparison to quantify the significance of the recognition of the different constructs.

Patients and control subjects

For the comparative analysis of MOG recognition by ELISA versus CBA we used serum samples from 18 patients with MOGAD (average age: 38 years, nine females, nine males). To set the threshold, we analysed 13 healthy donors. To set the threshold for our CBA we had included over the years 87 healthy controls (average age: 35 years, 53 females, 34 males). For the analysis of the recognition of MOG variants, we used serum samples and plasma samples of 14 patients with MOGAD (average age: 39 years, six females, eight males), who showed a strong MOG reactivity in the CBA including 12 patients from the above comparison (Fig. 1, filled circles). For comparison, one patient who scored negative in the CBA and the ELISA was included throughout (designated as C). Patients with MOG-Abs (Patients 5, 7, 10, 14, 16 and 17) were described in Spadaro et al.²⁶, and Patients 22, 23, 24, 38, 39, 41, 42 and 43 in

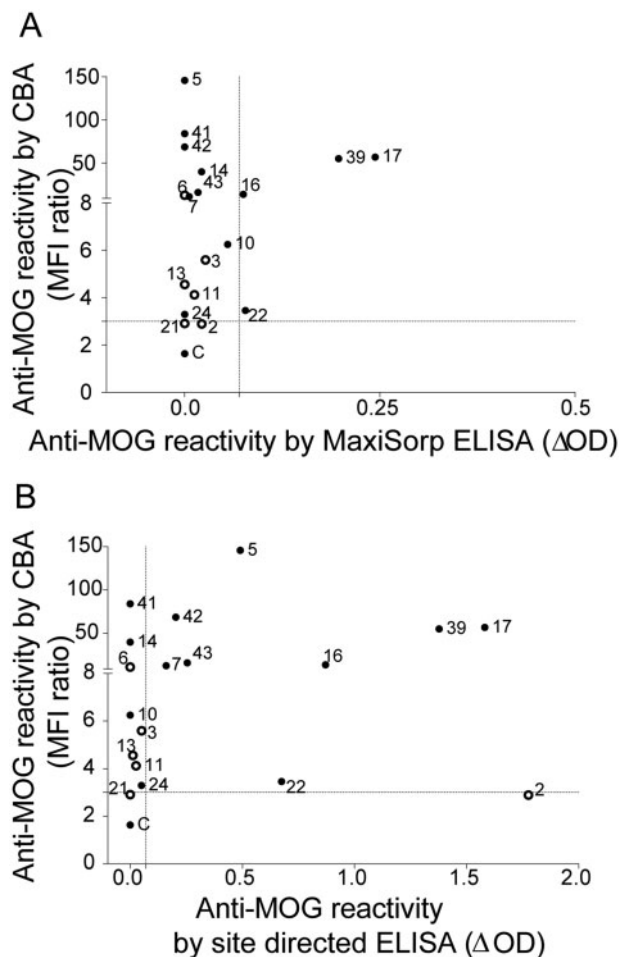


Figure 1 Comparison of MOG reactivity by ELISA and CBA. The anti-MOG reactivity of 18 patients with MOG-Abs was determined by CBA using FL-MOG and by ELISA. CBA was performed as described²⁶ and the anti-MOG reactivity is shown as MFI ratio, calculated as described in the ‘Materials and methods’ section. (A) For ELISA, MOG-1–125 was bound to MaxiSorp™ plates and Δ OD was calculated after subtraction of the OD of BSA-coated MaxiSorp™ plates. Alternatively, MOG-1–125 was biotinylated at its C-terminal Avi-tag and bound to streptavidin plates. (B) For ELISA, the anti-MOG reactivity is expressed as Δ OD (streptavidin + MOG) – (streptavidin only). The horizontal dashed lines represent the mean of the anti-MOG reactivity of a total of 87 healthy controls + 3 standard deviations (SD). The vertical dashed lines represent the mean + 3 SD of 13 healthy controls. Samples included in the analysis of recognition of MOG variants are indicated as filled circles.

Winklmeier et al.³⁴ Informed consent was obtained from each donor according to the Declaration of Helsinki and the ethical committee of the medical faculty of the LMU approved the study.

Data availability

The data presented in the manuscript are available from the corresponding author on request.

Results

MOG-1–125 displayed on an ELISA plate allows detection of MOG antibodies only in a few patients

The epitopes of MOG recognized by autoantibodies from patients are located in the loops that link the β -sheets of the extracellular

part of MOG.^{19,25} We produced this extracellular part in a correctly folded form and confirmed the β -sheet conformation by circular dichroism.^{24,26} We used this part of MOG for two ELISA variants. In one, MOG-1–125 was bound to typical MaxiSorp™ plates and in the other MOG-1–125 was enzymatically biotinylated at the Avi-tag of its C-terminus and bound in a site-directed manner to streptavidin plates. Both ELISAs were validated with r8-18C5 (Supplementary Fig. 1). We analysed 18 patients with MOG-Abs and compared the anti-MOG reactivity obtained by CBA using full-length MOG with the recognition of MOG by the two ELISA variants (Fig. 1). The MaxiSorp™ ELISA detected MOG-Abs in 4/18 patients, while the streptavidin-biotinylated MOG-ELISA detected 9/18 patients with MOG-Abs. Thus, an ELISA using site-directed binding of MOG-1–125 is superior to a random binding of MOG-1–125. However, even this improved ELISA did not detect half of the patients who scored positive in a CBA with MOG-transfected cells.

The C-terminus of MOG is intracellular

Since MOG-1–125 used in the ELISA assay had a sensitivity to detect MOG-Abs in patients’ sera, we specifically revisited whether the C-terminus of MOG (from amino acid 203 to 218) is intracellular or extracellular. We used ab28766, specific for the last 12 amino acids of MOG (Fig. 2A), and the mAb r8-18C5 that binds to a defined loop on the extracellular part of MOG around amino acid 103²¹ (Fig. 2A). Both antibodies were tested on HeLa cells transiently transfected with FL-MOG or ED-MOG tagged at the N-terminus with EYFP to ensure that the fluorescent tag did not interfere with the binding of the antibody to the C-terminus. Additionally, TE-671 (rhabdomyosarcoma) cells stably transfected with FL-MOG without any tag¹⁵ were used (Fig. 2B–I).

The mAb r8-18C5 bound to FL-MOG and ED-MOG in HeLa cells, as well as the FL-MOG in TE-671 cells, in both living and fixed conditions (Fig. 2B, C, F and G). In contrast, the ab28766 failed to detect MOG in both cell lines when living cells were analysed (Fig. 2D and H). However, once the cells (HeLa and TE671) were fixed and permeabilized, the ab28766 bound to EYFP-FL-MOG in HeLa cells and also to the FL-MOG stably expressed on the TE-671 cells (Fig. 2E and I). As a further control for the specificity of the applied antibodies, we used HeLa cells transfected with ED-MOG (lacking the C-terminus). These cells were not recognized by the ab28766, neither in the viable nor fixed and permeabilized conditions (Fig. 2D and E). We conclude that the C-terminus of the MOG protein is intracellular. Thus, the patient samples that recognized FL-MOG in live CBAs had bound to the N-terminal extracellular part of MOG.

Displaying MOG-1–125 in a fluid lipidic environment does not improve antibody detection

Having seen the drastic difference between MOG-1–125 bound to an ELISA plate and FL-MOG displayed on transfected cells, we tested the effect of embedding of MOG in a lipid environment on antibody recognition. Thus, we explored the impact of a fluid lipidic environment on the detection of ED-MOG, by designing a new assay.

We coated silica beads of dimensions similar to cells (6 μ m in diameter) with a lipid mixture that would mimic the lipid bilayer that forms the cell membrane (Fig. 3A). To monitor the lipid coating of the beads, the mixture contained fluorescently labelled lipids with Atto488 and biotinylated lipids for a neutravidin bridge to attach biotinylated MOG-1–125. The biotinylated MOG-1–125 was correctly folded as assessed by circular dichroism^{24,26} and was expected to move freely along the lipid bilayer when linked to the biotinylated lipid via neutravidin.³⁵ MOG-1–125, bound to lipid-coated beads, was detected by r8-18C5 (Fig. 3A, C and D). However,

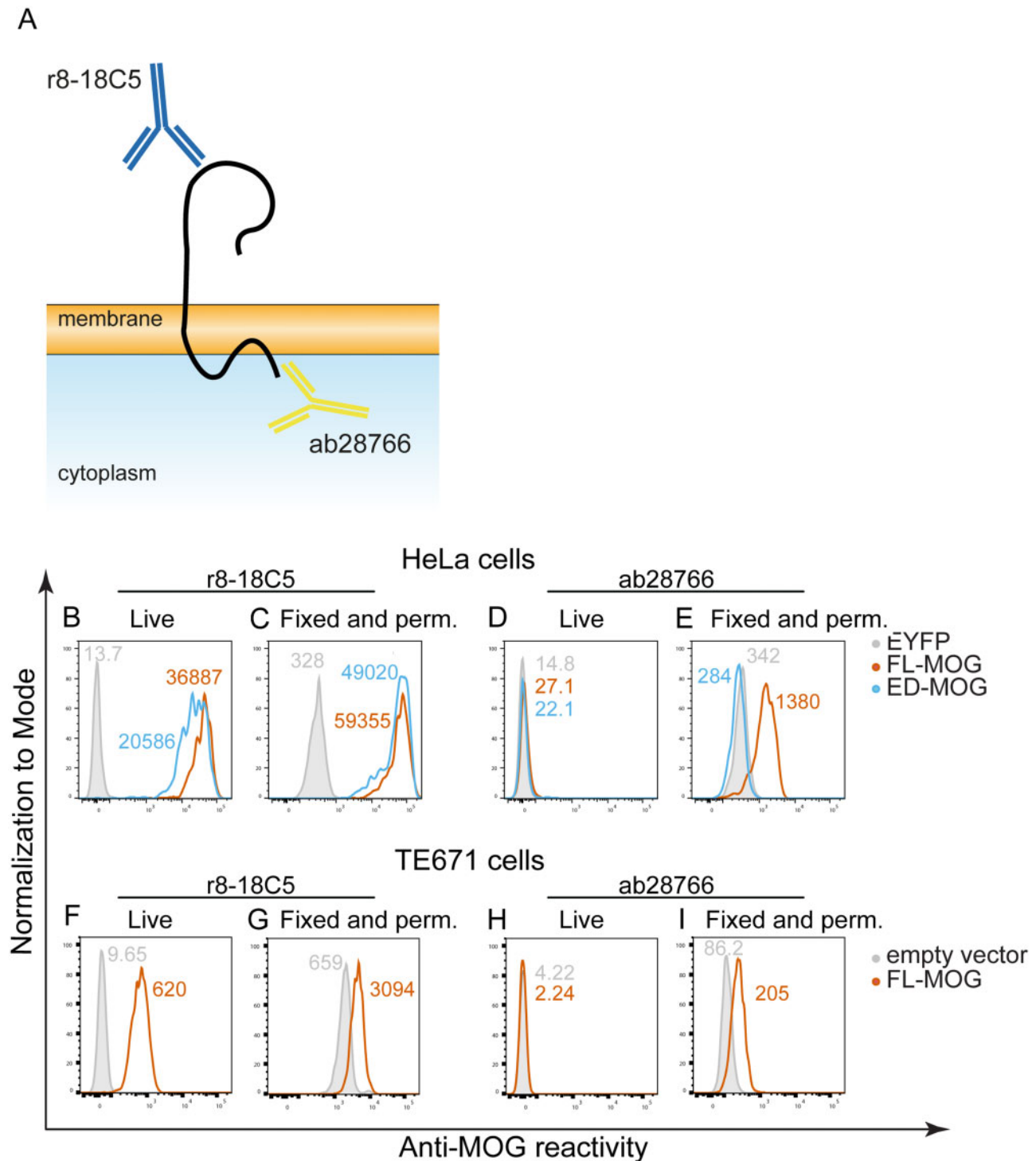


Figure 2 Localization of the C-terminus of MOG. (A) Schematic representation of the binding of the recombinant humanized r8-18C5 (blue) and ab28766 (yellow). (B–E) HeLa cells were transiently transfected with EYFP alone (closed grey graph), with FL-MOG (orange line), or ED-MOG (light blue line). FL-MOG and ED-MOG were fused to EYFP at the N-terminus. These cells were tested live (B and D) as well as after fixation and permeabilization (C and E) with r8-18C5 (B and C) and ab28766 (D and E). Gates were set to an EYFP signal > 100. (F–I) TE671 cells stably transfected with FL-MOG (orange line) or the empty vector (filled grey graph) were tested live (F and H) as well as after fixation and permeabilization (G and I) with r8-18C5 (F and G) and ab28766 (H and I). MFI values are given for each histogram.

the intensity of the binding was lower in comparison to FL-MOG or ED-MOG expressed in transiently transfected cells (Fig. 3D). We incubated these beads with sera of five patients (Patients 5, 14, 16, 17 and 22) (Fig. 3E). Three of these patients (Patients 5, 17 and 22) weakly recognized MOG displayed by these beads. Those three

patients were also detected by site-directed ELISA (Fig. 1B). Nevertheless, the MOG-1-125 in the site-directed ELISA was also capable of binding the antibodies of Patient 16. Therefore, we conclude that the embedding of MOG-1-125 in a fluid lipidic environment does not improve antibody detection.

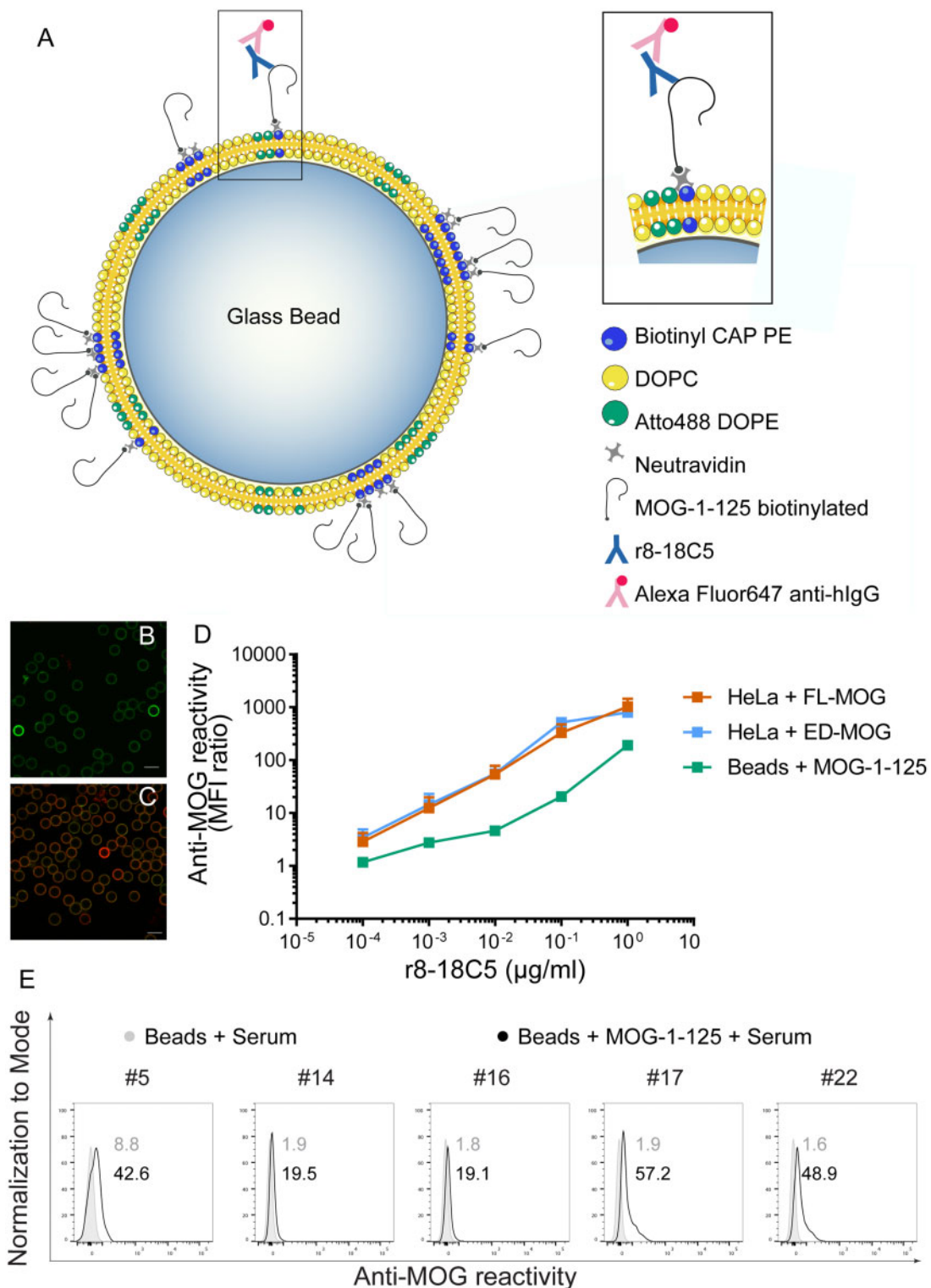


Figure 3 Detection of MOG-1-125 displayed on lipid-coated beads. (A) Schematic representation of the lipid-coated silica beads model. Glass beads (6 μm in diameter) were coated with a lipid mixture that formed a bilayer. The correctly folded MOG-1-125 is displayed on this bilayer. The magnification shows a segment of a single lipid-coated bead. Biotinylated MOG-1-125 is attached to the Biotinyl CAP PE via one of the free subunits of the neutravidin. MOG-1-125 is bound by the r8-18C5 (blue), which is detected by the Alexa Fluor® 647 anti-human IgG (magenta). (B and C) Confocal microscopy image of lipid-coated beads, to assess the extent of the coating. (B) The Atto488 DOPE lipids gave a green fluorescence to the whole membrane coating. (C) MOG displayed on these beads is detected by r8-18C5 and visualized with a red-labelled secondary antibody. B and C were taken with a 40 \times water objective. Scale bar = 10 μm . (D) Detection of increasing concentrations of r8-18C5 by cells transfected with FL-MOG (orange), ED-MOG (light blue line) and by lipid-coated beads displaying MOG-1-125 (dark green line). (E) Binding of sera (diluted 1:50) of five patients with MOG-Abs to MOG-1-125-coated beads. The closed grey graphs represent background bindings of the beads, the black line represents binding to beads displaying MOG-1-125. MFI values for each histogram are given.

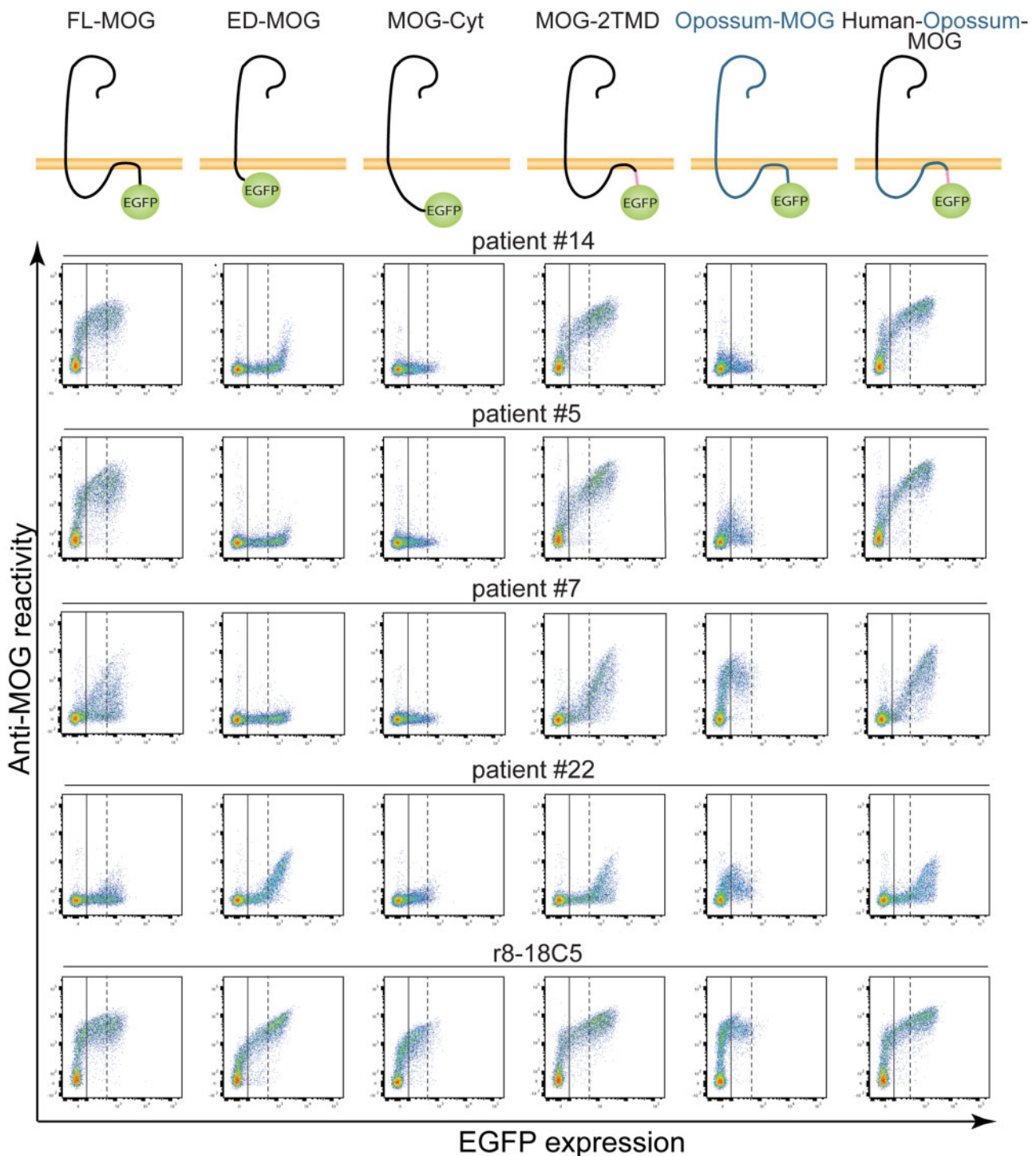


Figure 4 MOG variants used for transient transfection and their recognition by selected patients. Top row: Cartoons of MOG variants used. Rows 2–5 show dot plots obtained with serum diluted 1:50 of the indicated patients. Patients 14, 5, and 7 represent the majority of the patients, because they show a greater recognition of FL-MOG compared to ED-MOG. Patient 22 has an unusual binding behaviour, as it strongly recognizes ED-MOG. The bottom row shows the reactivity of the MOG-specific control mAb r8-18C5 (0.5 μ g/ml). The two vertical lines in each dot plot indicate an EGFP intensity of 100–500 (dotted) that is used as threshold for the quantitative analysis in Fig. 5.

The second hydrophobic domain of MOG is crucial for MOG recognition by most patients

We tested sera from 14 patients with MOG-Abs for recognition of HeLa cells transfected with FL-MOG or ED-MOG. For comparison, we also show the reactivity of one MOG negative patient (Patient C) to all of our mutants (Figs 4 and 5 and Supplementary Fig. 3). All

of the 14 MOG+ patients recognized FL-MOG much better than ED-MOG ($P < 0.0001$) (Fig. 5B). Figure 4 shows details of representative patients. Figure 5 and Supplementary Fig. 3 show the summary of all analysed patients and related statistics. Overall, only 5 of 14 MOG+ patients (36%) were detected by cells transfected with ED-MOG (Fig. 5A and Supplementary Fig. 3A). Thus, not only in the ELISA assay, but even in the CBA was ED-MOG poorly recognized

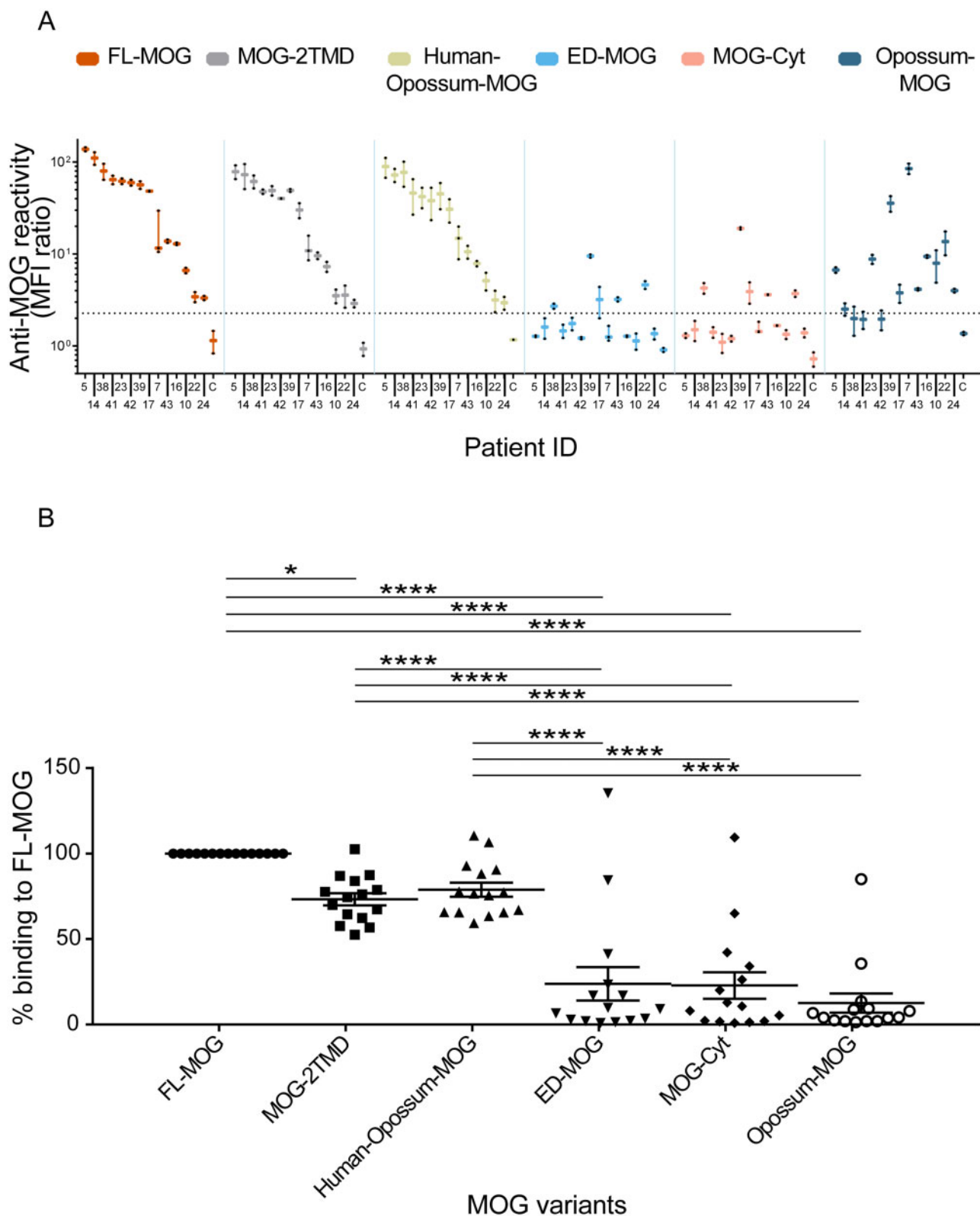


Figure 5 Differential detection of MOG variants and quantification. (A) Sera from 14 patients with MOG-Abs and one negative control (C) were tested for reactivity towards the six MOG variants. The mAb r8-18C5 (0.5 µg/ml) was used as a control. For the quantitative evaluation, the cells with EGFP signal between 100 and 500 were considered (Fig. 4). Error bars indicate standard error of the mean (SEM) of two experiments. (B) The reactivity of all the MOG variants normalized to FL-MOG (set as 100%) is shown with EGFP gating of 100–500. ED-MOG, MOG-Cyt and opossum-MOG were significantly less able to detect the MOG+ patients when compared with FL-MOG, MOG-2TMD and human-opossum MOG ($P < 0.0001$). The EGFP gating of 100–500 also highlights a difference in the reactivity between MOG-2TMD and FL-MOG ($P < 0.05$), but MOG-2TMD is still able to detect all 14 MOG+ patients.

by most patients, deeming it insufficient to detect MOG-Abs. The detailed recognition of epitopes of MOG was determined for 12 of 14 patients and they recognized different epitopes, as seen with point mutations of the loops linking the β -sheets of the N-terminal part of MOG (Supplementary Fig. 5). Thus, the strong recognition of FL-MOG as compared to ED-MOG is not related to certain epitopes on the extracellular part of MOG, but is rather a general feature of MOG-Abs from patients.

We went on to narrow down the intracellular domains of MOG, which increase the antibody detection of the extracellular domain. Hence, we designed two MOG variants. The first is composed of the extracellular part, the first transmembrane domain and the cytoplasmic part until the second hydrophobic domain (Tyr181), named MOG-Cyt (Fig. 4). Second, we cloned a longer variant of MOG that included the second hydrophobic domain (to leucine-202), called MOG-2TMD (Fig. 4). These variants were tested for recognition by autoantibodies from our 14 patients (Fig. 5 and Supplementary Fig. 3).

The raw data in the dot plots already indicate that the three representative Patients 5, 7 and 14 strongly recognized MOG-2TMD, but MOG-Cyt only weakly (Fig. 4). Considering all patients, MOG-Cyt was far less recognized than MOG-2TMD or FL-MOG ($P < 0.0001$) (Fig. 5 and Supplementary Fig. 3A). In particular, the reactivity towards MOG-Cyt dropped in 13/14 patients, even below 20% compared to FL-MOG (Fig. 5B). Together, this part of our analysis identified the second hydrophobic domain of MOG as the crucial non-extracellular part of MOG to enhance recognition of its extracellular part by autoantibodies from patients.

To elaborate the impact of the second hydrophobic part of MOG for antigen recognition, we analysed the recognition of FL-MOG from the evolutionary distant opossum (*Monodelphis domestica*) and of a chimeric construct composed of the extracellular and first hydrophobic domain of human MOG fused to the cytoplasmic and second hydrophobic domain from opossum (Fig. 4). The group of patients with MOG-Abs recognized opossum MOG weaker than human FL-MOG ($P < 0.0001$) (Fig. 5A). We also observed a heterogeneous recognition of opossum-MOG by patients: compared to human FL-MOG, of 14 MOG+ patients, seven showed a weak cross-reactivity to opossum-MOG (recognition $< 20\%$). Two patients recognized it similarly (Patients 39 and 10), and another two (Patients 7 and 22) recognized the opossum-MOG even better than the human MOG (Fig. 4 and Supplementary Fig. 3). Strikingly, the human opossum construct was detected by all 14 MOG+ patients. Of note, the four patients (Patients 14, 38, 41 and 42) who did not show cross-reactivity to opossum MOG had also detected the human-opossum construct (Fig. 5 and Supplementary Fig. 3A). Human-opossum MOG was better recognized than ED-MOG by all 14 patients ($P < 0.0001$) (Supplementary Fig. 3A). Thus, the intracellular part of opossum-MOG greatly enhances recognition of the extracellular part of human MOG. In contrast to patients with MOG-Abs, the mAb r8-18C5 recognized all MOG variants similarly, as elaborated in a dose-response (Supplementary Fig. 4).

MOG-Abs affinity-purified with the extracellular part of MOG still preferentially recognize full-length MOG

We affinity-purified MOG-Abs using MOG-1–125 from Patient 7, who showed a typical and strong recognition of FL-MOG while a weak recognition of ED-MOG (Fig. 4). Remarkably, not only the serum antibodies, but also the MOG-Abs affinity-purified with the recombinantly produced MOG-1–125 recognized FL-MOG much better than ED-MOG in transfected cells. (Supplementary Fig. 6A). We noted that this type of affinity purification does not extract all MOG-Abs; a substantial amount were still present in the flow-

through. We compared the affinity-purified antibodies with the starting material (plasma) and the flow-through with respect to recognition of mutated variants of the extracellular part of MOG, which are known to identify MOG epitopes.²⁵ This showed that the MOG-Abs that were affinity-purified with the ED-MOG recognized the same epitopes on the extracellular part of MOG as the crude plasma and as the antibodies in the flow-through (Supplementary Fig. 6B). Together, these experiments indicate that MOG-Abs of the same antigenic immunoreactivity within one patient strongly recognize FL-MOG and weakly ED-MOG.

Bivalent recognition of MOG required by antibodies from patients

We analysed the importance of bivalent binding for the differential recognition of FL-MOG and ED-MOG. To this end, with pepsin and papain digestion, we generated Fab and F(ab')₂ fragments of the r8-18C5 as well as IgGs of four patients (Patients 14, 16, 17 and 22). We picked a highly reactive MOG patient (Patient 14), one medium reactive patient (Patient 16), one patient whose antibodies were also detected in the ELISA assay (Patient 17) (Fig. 1), and Patient 22, whose antibodies were also detected by ELISA and bound strongly to ED-MOG and FL-MOG (Fig. 4). F(ab')₂ fragments were obtained by pepsin digestion; F(ab) fragments were obtained by digestion with papain and subsequent size exclusion chromatography to separate the undigested pool of antibodies from the Fab fragments (Fig. 6A).

We compared the reactivities of Fab and F(ab')₂ fragments on cells transfected with FL-MOG or ED-MOG. The F(ab')₂ fragments from the four patients behaved in the same manner as the purified IgGs (Fig. 6B). The Fab preparations of all four analysed patients showed little or no recognition of either FL-MOG or ED-MOG (Fig. 6B). In contrast, the Fab from r8-18C5 clearly bound to both FL-MOG and ED-MOG. A dose response of r8-18C5 and its Fab and F(ab')₂ fragments demonstrated that the recognition of Fab is slightly weaker than of F(ab')₂, but Fab and F(ab')₂ of this mAb did not differentiate between FL-MOG and ED-MOG (Supplementary Fig. 7). Together, this illustrates that MOG-Abs from patients, but not the mAb r8-18C5, strictly require bivalent recognition to bind to MOG. The need for bivalent binding and the importance of the second hydrophobic are presented in our model in Fig. 7.

Förster resonance energy transfer does not show dimerization of ED-MOG or FL-MOG

We investigated whether FL-MOG or ED-MOG formed dimers detected by FRET. To this end, we co-transfected HEK-293T cells with ECFP-FL-MOG and EYFP-FL-MOG or with ECFP-ED-MOG and EYFP-ED-MOG. These experiments revealed that neither FL-MOG nor ED-MOG came so close to each other that this would result in a FRET signal. In contrast, the positive control, fusion protein ECFP-EYFP yielded a strong FRET signal (Supplementary Fig. 8).

Discussion

We report that the second hydrophobic domain of MOG enhances recognition of its N-terminal extracellular part in most patients and propose that this is the reason why a CBA with FL-MOG is the gold standard to identify patients with MOG-Abs. Most MOG-Abs from patients recognize loops that link the β -sheets of the IgV-like fold of the extracellular N-terminal part of MOG.²⁵ This part of MOG (MOG-1–125) can be produced in a conformationally correctly folded way,^{19,24,26} but this is not sufficient to identify MOG-Ab-positive patients. This was seen in a recent study, where MOG was bound in a random way to an ELISA plate.¹⁹ Our study confirms this and shows that a site-directed display of MOG on the ELISA is

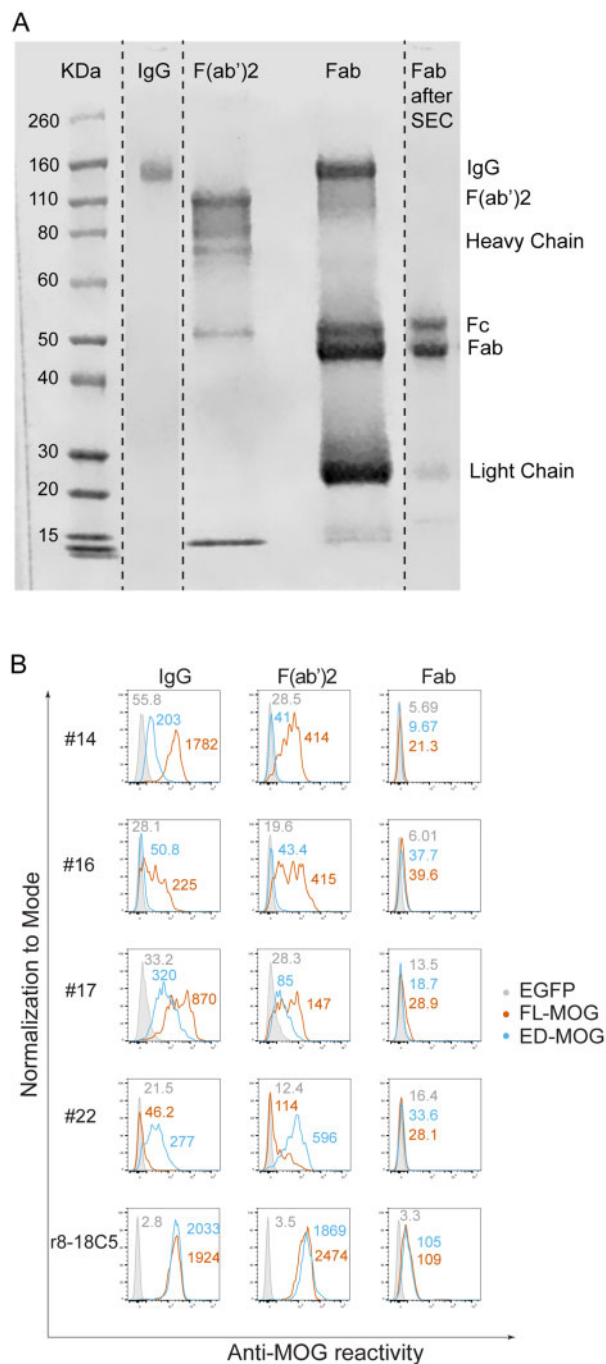


Figure 6 Recognition of FL-MOG and ED-MOG by F(ab')₂ and Fab preparations. (A) Preparation of F(ab')₂ and Fab. IgGs purified with protein-G columns were digested with pepsin to obtain the F(ab')₂ and with papain to yield Fab. Since the Fab preparations obtained after papain digestion still contained undigested IgG, the Fab fragments were further purified by size exclusion chromatography (SEC). Elution fractions were separated by non-reducing SDS-PAGE and stained with Coomassie. Relevant elution fractions were then pooled and analysed again on an SDS-PAGE gel. Here, Patient 14 is shown as a representative example. (B) HeLa cells were transfected with EGFP, FL-MOG or ED-MOG. Binding of IgGs from plasma (400 µg/ml), F(ab')₂ (800 µg/ml) and Fab (800 µg/ml) of the indicated patients was determined with secondary antibodies specific for Ig-kappa and Ig-lambda, as described in the 'Materials and methods' section. The mAb r8-18C5 (0.1 µg/ml) was used as a control. The anti-MOG reactivities were calculated on transfected cells with EGFP signal >500. MFI values are given for each histogram. Representative measurements from two experiments with similar results are shown.

superior, but still insufficient to identify all patients with MOG-Abs.

We found that MOG-1–125 embedded in a fluidic lipid environment is recognized by the anti-MOG mAb r8-18C5 and weakly by patients, but far less efficient than MOG in transfected cells. Therefore, we worked out details of MOG recognition in transfected cells and found that most patients recognized FL-MOG much better than ED-MOG. This is in accordance with a previous report.³⁰ We went on to dissect the contribution of the intracellular part of MOG for the enhanced recognition of FL-MOG with different truncated variants of MOG and this revealed that the second hydrophobic domain of MOG is crucial for the detection of MOG by patients with MOG-Abs.

We continued to analyse whether this enhanced recognition of MOG by the intracellular part is based on a specific sequence of MOG or rather based on the overall structure of MOG. While wrapped myelin is found in vertebrates, MOG is found only in mammals. We expressed MOG from opossum, the evolutionarily most distant animal from whom a MOG sequence was available in the NCBI database. Most patients did not or only weakly recognized MOG from opossum. This was expected, since many patients do not even show cross-reactivity to rodent MOG.^{25,26,36} Importantly, when we constructed a chimeric MOG, with the N-terminal ED part from human MOG and the C-terminal part from opossum MOG, this MOG construct was recognized as strongly as the full-length human MOG. We observed this enhanced recognition of MOG by the second transmembranous domain of MOG in patients who recognized different epitopes on the extracellular part of MOG (Supplementary Fig. 5). This argues that the second hydrophobic domain does not induce the exposure of a specific epitope, but induces an overall structure of MOG that is better recognized by autoantibodies.

We tested whether the enormous difference in recognition of ED-MOG versus FL-MOG could be attributed at least partially to an extracellular display of the C-terminal part of MOG. All of our experiments using both transiently and stably transfected cells came to the same conclusion, namely that the C-terminus is intracellular. Our observation is in line with earlier reports,^{27,28} but at variance with the current prediction of UniProt (27 November 2020), and a model presented in a recent review with reference to UniProt.²⁹ Our model in Fig. 7 includes the specific amino acid composition of the second hydrophobic domain of MOG and their adjacent amino acids: the second hydrophobic domain has two prolines. A proline might indicate a kink in the α -helix.^{37,38} A similar monotopic domain displaying an analogous structure with two hydrophobic helices and a proline in the middle (helix-break-helix) is also seen for caveolin³⁹ and for the transmembrane protein PEN-2, a subunit of the Alzheimer's disease and Notch signalling-related protease γ -secretase.^{40,41} Also, the three positively charged amino acids next to the hydrophobic domain that were expected to bind to negatively charged lipids intracellularly and the cysteine at the end of the hydrophobic domain that might be palmitoylated⁴² are linked to the intracellular localization of the C-terminus of MOG. These four amino acids are also conserved from opossum to human (Supplementary Fig. 9). Further, we found that all patients with MOG-Abs recognized the mutant MOG-2TMD, which does not include the C-terminus, at least as strongly as FL-MOG. Together, this part of our study established that the C-terminus of MOG is intracellular and in contrast to the second hydrophobic domain, not involved in binding of patient antibodies to FL-MOG.

To gain further insight into the details of MOG recognition, we analysed whether FL-MOG or ED-MOG form close dimers detectable by FRET, and analysed monovalent versus bivalent binding to FL-MOG and ED-MOG. We found that neither ED-MOG nor FL-MOG gave a FRET signal. The intensity of a FRET signal is inversely

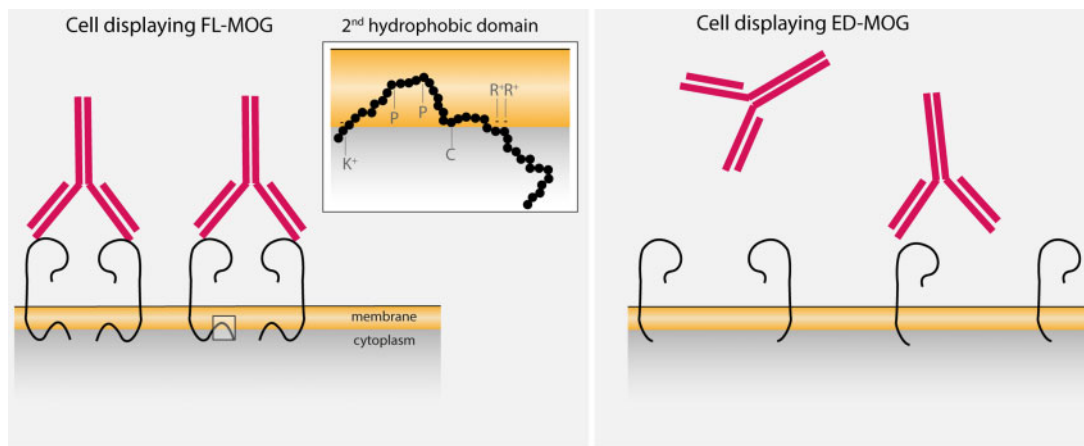


Figure 7 Model illustrating how the second hydrophobic domain of MOG enhances recognition of its extracellular part by autoantibodies from patients. We show in this paper that MOG-Abs from patients require bivalent binding and the second hydrophobic domain for MOG binding. We therefore propose the model shown here in which the second hydrophobic domain of MOG facilitates bivalent binding of MOG-Abs. The magnified figure shows how the second hydrophobic domain is embedded in the membrane in a monotopic manner with both sides of this hydrophobic domain in the cytoplasm. The two prolines (P) in the middle induce kinks inside the membrane. Positively charged amino acids arginine (R) and lysine (K) adjacent to the hydrophobic domain might interact with the cytosolic interface of the membrane. The cysteine (C) at the end of the hydrophobic domain might be palmitoylated. The presence of the second hydrophobic domain brings MOG molecules to a distance that allows bivalent binding of autoantibodies. The absence of the second hydrophobic domain in the ED-MOG protein leads to the weak and monovalent binding of MOG-Abs.

proportional to the sixth power of the inter-dye distance and this energy transfer process can serve as a spectroscopic ruler in the 1–6 nm range.⁴³ Thus, our FRET experiments show that ED-MOG and FL-MOG are further apart from each other than 6 nm. To allow bivalent binding of IgG1 (the typical isotype of MOG-Abs), the target antigen has to be at a relatively strict distance of ~13–16 nm, as recently corroborated with DNA origami technology.⁴⁴ In a crystallographic paper, ED-MOG was reported to form a head-to-tail dimer²²; in the same report, MOG extracted from myelin appeared largely monomeric by western blot, but also a small proportion of dimeric forms of MOG were observed, indicating that MOG may form dimers under special crystallization conditions and also in myelin. Our FRET experiments do not exclude dimer formation of MOG under certain situations, but show that under our experimental conditions, cells transfected with MOG for a CBA, MOG does not associate closer than 6 nm. In accordance with our FRET data, MOG from transfected cells appeared as a monomer when western blots of transfected cells were performed.^{24,25}

We found that MOG-Abs from four patients bound strongly in the form of F(ab)₂, but poorly or not at all as Fab, indicating that these MOG-Abs largely require bivalent binding to be detected. The dependence on bivalent binding is most likely due to concentration and affinity. In particular, it argues that the affinity of human MOG-Abs is lower than of 8-18C5 and therefore a gain of avidity due to bivalent binding is needed for a clear binding to MOG. Also, *in vitro* translated extracellular part of MOG constructed to form tetramers is recognized by MOG-Abs from patients.¹² We speculate that FL-MOG is better recognized than ED-MOG, because the intracellular part of MOG induces a clustering of MOG with a spacing of the extracellular part of MOG that allows bivalent antibody binding, as illustrated in Fig. 7. The second hydrophobic domain could hold the monomers apart at a suitable distance that would facilitate the bivalent binding of the MOG-Abs, presumably involving lipid rafts.⁴⁵ This model is in accordance with previous studies that showed that crosslinking of MOG-Abs induces signalling⁴⁶ and lateral diffusion of transfected MOG in the membrane is anomalous and slowed down.^{47,48} We are aware that our model in Fig. 7 might not be the only possible explanation for the enhanced recognition and bivalent binding of MOG-Abs when the second hydrophobic domain is present. It could also be that the second

hydrophobic domain creates an empty space around the MOG molecules, which favours the binding of MOG-Abs.

We assume that the few patients whose MOG-Abs gave some signal using MOG-1–125 bound to an ELISA plate or to ED-MOG in transfected cells, have such a strong affinity that allows monovalent binding. This view is also strengthened by features of the mAb r8-18C5, which has a strong affinity to MOG, binds also as Fab to MOG, recognizes ED-MOG and FL-MOG in transfected cells similarly and also MOG by ELISA. Together, we show that MOG-Abs from most patients require bivalent binding to be detected. We propose that bivalent binding is facilitated with cells transfected with FL-MOG (or MOG-2TMD), but not when ED-MOG is transfected or when MOG-1–125 is bound to an ELISA plate.

Patients with antibodies to MOG or AQP4 show clinically overlapping features, but consensus is emerging that anti-MOG and anti-AQP4 constitute separate diseases.^{5,9,49} While this study indicates that MOG-Abs from most patients require bivalent binding for antigen-recognition, autoantibodies to AQP4 have been reported to also bind as monomer.⁵⁰ Monovalent binding of IgG provides a more efficient platform for C1q binding and complement activation than bivalent binding.^{51,52} Previous work has shown that complement-mediated activation by MOG-Abs *in vitro* was restricted to high-titre positive patients.⁵³ Thus, MOG-Abs may activate complement, but they do this far less efficiently than by AQP4-Abs. This view is supported by histopathological examinations: although C9neo deposition can be observed in patients with MOG-Abs^{54–57} or after transfer of their MOG-Abs,²⁶ it is far less pronounced than in patients with antibodies to AQP4.^{7,58,59} In particular, patients with AQP4-Abs have large perivascular complement deposition that is missing in MOGAD.^{5,8}

While IgGs from patients with AQP4-Abs readily induce disease upon transfer,⁵⁸ this has been difficult to achieve with IgG preparations from MOG-Ab-positive patients and it took affinity purification of antibodies from selected patients to achieve this.²⁶ These affinity-purified antibodies that transfer disease also recognize MOG by ELISA, as shown here. Recognition of MOG by ELISA by a few patients was interpreted as an indicator of high affinity,¹⁹ suggesting that these patients' antibodies might bind monovalently. Along this line, only a single patient with high-titre antibodies to MOG was able to induce complement-dependent tissue injury in

an *ex vivo* organotypic brain slice model³⁶ and no complement-dependent changes were observed upon intracerebral injection of pooled IgG from MOG-positive patients.⁶⁰ Complement-independent pathomechanisms of MOG-Abs include also cytoskeletal alterations⁶¹ and antibody-mediated cellular cytotoxicity.¹³

The observations from pathology and our finding that MOG-Abs largely bind bivalently have therapeutic implications. This suggests that the anticomplement therapy with eculizumab, which is very successful in patients with anti-AQP4,⁴⁰ might be less effective in patients with MOG-Abs. Autoantibodies may induce pathology by multiple mechanisms other than complement activation, including endocytosis and FcR activation.^{2,62} In animal models of haemolytic anaemia, low-affinity bivalently binding autoantibodies were highly pathogenic.⁶³ MOG-Abs affinity-purified from patients were pathogenic by enhancing activation of cognate T cells,²⁶ presumably by accumulating in CNS-resident phagocytes⁶⁴ and enhancing T-cell activation via FcR-dependent opsonization of MOG.⁶⁵

Together, we report that MOG-Abs from most patients require the intracellular part of MOG to recognize its extracellular part and show a bivalent binding to MOG. These features of human MOG-Abs explain why a CBA with FL-MOG is the gold standard to identify such patients and have implications for our concept about pathogenicity of human MOG-Abs.

Acknowledgements

We are grateful to Heike Rübsamen for technical assistance and Prof. Hartmut Wekerle for the continuous support. We are grateful to Prof. Hermann Eibel for kindly providing the FRET control constructs. We thank Samantha Ho together with Drs Naoto Kawakami and Klaus Dornmair for comments on the manuscript. FRET experiments were supported by Dr L. Richter, Core Facility Flow Cytometry at the Biomedical Center, LMU Munich.

Funding

This study was funded by the DFG (SFB TR128) and under Germany's Excellence Strategy within the framework of the Munich Cluster for Systems Neurology (EXC 2145 SyNergy– ID 390857198), the Werner Reichenberger Stiftung, the Verein zur Therapieforschung für MS-Kranke, the Alexander von Humboldt Foundation and the TUBITAK 2219 program.

Competing interests

The authors report no competing interests.

Supplementary material

Supplementary material is available at *Brain* online.

References

- Brimberg L, Mader S, Fujieda Y, et al. Antibodies as mediators of brain pathology. *Trends Immunol.* 2015;36(11):709–724.
- Dalmau J, Graus F. Antibody-mediated encephalitis. *N Engl J Med.* 2018;378(9):840–851.
- Durozard P, Rico A, Boutiere C, et al. Comparison of the response to rituximab between myelin oligodendrocyte glycoprotein and aquaporin-4 antibody diseases. *Ann Neurol.* 2020;87(2):256–266.
- Jurynczyk M, Messina S, Woodhall MR, et al. Clinical presentation and prognosis in MOG-antibody disease: A UK study. *Brain.* 2017;140(12):3128–3138.
- Mader S, Kumpfel T, Meinl E. Novel insights into pathophysiology and therapeutic possibilities reveal further differences between AQP4-IgG- and MOG-IgG-associated diseases. *Curr Opin Neurol.* 2020;33(3):362–371.
- Reindl M, Waters P. Myelin oligodendrocyte glycoprotein antibodies in neurological disease. *Nat Rev Neurol.* 2019;15(2):89–102.
- Takai Y, Misu T, Kaneko K, et al.; the Japan MOG-antibody Disease Consortium. Myelin oligodendrocyte glycoprotein antibody-associated disease: An immunopathological study. *Brain.* 2020;143(5):1431–1446.
- Weber MS, Derfuss T, Metz I, Bruck W. Defining distinct features of anti-MOG antibody associated central nervous system demyelination. *Ther Adv Neurol Disord.* 2018;11:1756286418762083.
- Zamvil SS, Slavin AJ. Does MOG Ig-positive AQP4-seronegative opticospinal inflammatory disease justify a diagnosis of NMO spectrum disorder? *Neurol Neuroimmunol Neuroinflamm.* 2015;2(1):e62.
- Genain CP, Nguyen MH, Letvin NL, et al. Antibody facilitation of multiple sclerosis-like lesions in a nonhuman primate. *J Clin Invest.* 1995;96(6):2966–2974.
- Linnington C, Bradl M, Lassmann H, Brunner C, Vass K. Augmentation of demyelination in rat acute allergic encephalomyelitis by circulating mouse monoclonal antibodies directed against a myelin/oligodendrocyte glycoprotein. *Am J Pathol.* 1988;130(3):443–454.
- O'Connor KC, McLaughlin KA, De Jager PL, et al. Self-antigen tetramers discriminate between myelin autoantibodies to native or denatured protein. *Nat Med.* 2007;13(2):211–217.
- Brilof F, Dale RC, Selter RC, et al. Antibodies to native myelin oligodendrocyte glycoprotein in children with inflammatory demyelinating central nervous system disease. *Ann Neurol.* 2009;66(6):833–842.
- McLaughlin KA, Chitnis T, Newcombe J, et al. Age-dependent B cell autoimmunity to a myelin surface antigen in pediatric multiple sclerosis. *J Immunol.* 2009;183(6):4067–4076.
- Pröbstel AK, Dornmair K, Bittner R, et al. Antibodies to MOG are transient in childhood acute disseminated encephalomyelitis. *Neurology.* 2011;77(6):580–588.
- Litzenburger T, Fässler R, Bauer J, et al. B lymphocytes producing demyelinating autoantibodies: Development and function in gene-targeted transgenic mice. *J Exper Med.* 1998;188(1):169–180.
- Pollinger B, Krishnamoorthy G, Berer K, et al. Spontaneous relapsing-remitting EAE in the SJL/J mouse: MOG-reactive transgenic T cells recruit endogenous MOG-specific B cells. *J Exper Med.* 2009;206(6):1303–1316.
- Brehm U, Piddlesden SJ, Gardinier MV, Linnington C. Epitope specificity of demyelinating monoclonal autoantibodies directed against the human myelin oligodendrocyte glycoprotein (MOG). *J Neuroimmunol.* 1999;97(1-2):9–15.
- Tea F, Lopez JA, Ramanathan S, et al.; Australasian and New Zealand MOG Study Group. Characterization of the human myelin oligodendrocyte glycoprotein antibody response in demyelination. *Acta Neuropathol Commun.* 2019;7(1):145.
- Reindl M, Schanda K, Woodhall M, et al. International multicenter examination of MOG antibody assays. *Neurol Neuroimmunol Neuroinflamm.* 2020;7(2):e674.
- Breithaupt C, Schubart A, Zander H, et al. Structural insights into the antigenicity of myelin oligodendrocyte glycoprotein. *Proc Natl Acad Sci U S A.* 2003;100(16):9446–9451.
- Clements CS, Reid HH, Beddoe T, et al. The crystal structure of myelin oligodendrocyte glycoprotein, a key autoantigen in multiple sclerosis. *Proc Natl Acad Sci U S A.* 2003;100(19):11059–11064.

23. Breithaupt C, Schafer B, Pellkofer H, Huber R, Linington C, Jacob U. Demyelinating myelin oligodendrocyte glycoprotein-specific autoantibody response is focused on one dominant conformational epitope region in rodents. *J Immunol.* 2008;181(2):1255–1263.
24. Marti Fernandez I, Macrini C, Krumbholz M, et al. The glycosylation site of myelin oligodendrocyte glycoprotein affects autoantibody recognition in a large proportion of patients. *Front Immunol.* 2019;10:1189.
25. Mayer MC, Breithaupt C, Reindl M, et al. Distinction and temporal stability of conformational epitopes on myelin oligodendrocyte glycoprotein recognized by patients with different inflammatory central nervous system diseases. *J Immunol.* 2013;191(7):3594–3604.
26. Spadaro M, Winklmeier S, Beltran E, et al. Pathogenicity of human antibodies against myelin oligodendrocyte glycoprotein. *Ann Neurol.* 2018;84(2):315–328.
27. della Gaspera B, Pham-Dinh D, Roussel G, Nussbaum JL, Dautigny A. Membrane topology of the myelin/oligodendrocyte glycoprotein. *Eur J Biochem.* 1998;258(2):478–484.
28. Kroepfl JF, Viise LR, Charron AJ, Linington C, Gardinier MV. Investigation of myelin/oligodendrocyte glycoprotein membrane topology. *J Neurochem.* 1996;67(5):2219–2222.
29. Sinmaz N, Nguyen T, Tea F, Dale RC, Brilot F. Mapping autoantigen epitopes: Molecular insights into autoantibody-associated disorders of the nervous system. *J Neuroinflamm.* 2016;13(1):219.
30. Waters P, Woodhall M, O'Connor KC, et al. MOG cell-based assay detects non-MS patients with inflammatory neurologic disease. *Neurol Neuroimmunol Neuroinflamm.* 2015;2(3):e89.
31. Smulski CR, Decossas M, Chekkat N, et al. Hetero-oligomerization between the TNF receptor superfamily members CD40, Fas and TRAILR2 modulate CD40 signalling. *Cell Death Dis.* 2017;8(2):e2601.
32. Perera NC, Wiesmuller KH, Larsen MT, et al. NSP4 is stored in azurophil granules and released by activated neutrophils as active endoprotease with restricted specificity. *J Immunol.* 2013;191(5):2700–2707.
33. Brändle SM, Obermeier B, Senel M, et al. Distinct oligoclonal band antibodies in multiple sclerosis recognize ubiquitous self-proteins. *Proc Natl Acad Sci U S A.* 2016;113(28):7864–7869.
34. Winklmeier S, Schluter M, Spadaro M, et al. Identification of circulating MOG-specific B cells in patients with MOG antibodies. *Neurol Neuroimmunol Neuroinflamm.* 2019;6(6):625.
35. Ramm B, Glock P, Mucksch J, et al. The MinDE system is a generic spatial cue for membrane protein distribution in vitro. *Nat Commun.* 2018;9(1):3942.
36. Peschl P, Schanda K, Zeka B, et al. Human antibodies against the myelin oligodendrocyte glycoprotein can cause complement-dependent demyelination. *J Neuroinflamm.* 2017;14(1):208.
37. Nilsson I, Saaf A, Whitley P, Gafvelin G, Waller C, von Heijne G. Proline-induced disruption of a transmembrane alpha-helix in its natural environment. *J Mol Biol.* 1998;284(4):1165–1175.
38. von Heijne G. Proline kinks in transmembrane alpha-helices. *J Mol Biol.* 1991;218(3):499–503.
39. Aoki S, Thomas A, Decaffmeyer M, Brasseur R, Epanand RM. The role of proline in the membrane re-entrant helix of caveolin-1. *J Biol Chem.* 2010;285(43):33371–33380.
40. Pittock SJ, Berthele A, Fujihara K, et al. Eculizumab in aquaporin-4-positive neuromyelitis optica spectrum disorder. *N Engl J Med.* 2019;381(7):614–625.
41. Zhou R, Yang G, Guo X, Zhou Q, Lei J, Shi Y. Recognition of the amyloid precursor protein by human gamma-secretase. *Science.* 2019;363(6428):eaaw0930.
42. Smotrys JE, Linder ME. Palmitoylation of intracellular signaling proteins: Regulation and function. *Annu Rev Biochem.* 2004;73:559–587.
43. Stryer L, Haugland RP. Energy transfer: A spectroscopic ruler. *Proc Natl Acad Sci U S A.* 1967;58(2):719–726.
44. Shaw A, Hoffecker IT, Smyrlaki I, et al. Binding to nanopatterned antigens is dominated by the spatial tolerance of antibodies. *Nat Nanotechnol.* 2019;14(2):184–190.
45. Kim T, Pfeiffer SE. Myelin glycosphingolipid/cholesterol-enriched microdomains selectively sequester the non-compact myelin proteins CNP and MOG. *J Neurocytol.* 1999;28(4-5):281–293.
46. Marta CB, Montano MB, Taylor CM, Taylor AL, Bansal R, Pfeiffer SE. Signaling cascades activated upon antibody cross-linking of myelin oligodendrocyte glycoprotein: Potential implications for multiple sclerosis. *J Biol Chem.* 2005;280(10):8985–8993.
47. Gielen E, Smisdom N, De Clercq B, et al. Diffusion of myelin oligodendrocyte glycoprotein in living OLN-93 cells investigated by raster-scanning image correlation spectroscopy (RICS). *J Fluoresc.* 2008;18(5):813–819.
48. Gielen E, Vercammen J, Sýkora J, et al. Diffusion of sphingomyelin and myelin oligodendrocyte glycoprotein in the membrane of OLN-93 oligodendroglial cells studied by fluorescence correlation spectroscopy. *C R Biol.* 2005;328(12):1057–1064.
49. Fujihara K. Neuromyelitis optica spectrum disorders: Still evolving and broadening. *Curr Opin Neurol.* 2019;32(3):385–394.
50. Crane JM, Lam C, Rossi A, Gupta T, Bennett JL, Verkman AS. Binding affinity and specificity of neuromyelitis optica autoantibodies to aquaporin-4 M1/M23 isoforms and orthogonal arrays. *J Biol Chem.* 2011;286(18):16516–16524.
51. Diebold CA, Beurskens FJ, de Jong RN, et al. Complement is activated by IgG hexamers assembled at the cell surface. *Science.* 2014;343(6176):1260–1263.
52. Soltys J, Liu Y, Ritchie A, et al. Membrane assembly of aquaporin-4 autoantibodies regulates classical complement activation in neuromyelitis optica. *J Clin Invest.* 2019;129(5):2000–2013.
53. Mader S, Gredler V, Schanda K, et al. Complement activating antibodies to myelin oligodendrocyte glycoprotein in neuromyelitis optica and related disorders. *J Neuroinflamm.* 2011;8:184.
54. Hoftberger R, Guo Y, Flanagan EP, et al. The pathology of central nervous system inflammatory demyelinating disease accompanying myelin oligodendrocyte glycoprotein autoantibody. *Acta Neuropathol.* 2020;139:875–892.
55. Jarius S, Metz I, König FB, et al. Screening for MOG-IgG and 27 other anti-glial and anti-neuronal autoantibodies in 'pattern II multiple sclerosis' and brain biopsy findings in a MOG-IgG-positive case. *Mult Scler.* 2016;22:1541–1549.
56. Kortvelyessy P, Breu M, Pawlitzki M, et al. ADEM-like presentation, anti-MOG antibodies, and MS pathology: TWO case reports. *Neurol Neuroimmunol Neuroinflamm.* 2017;4(3):e335.
57. Spadaro M, Gerdes LA, Mayer MC, et al. Histopathology and clinical course of MOG-antibody associated encephalomyelitis. *Ann Clin Transl Neurol.* 2015;2:295–301.
58. Bradl M, Mitsu T, Takahashi T, et al. Neuromyelitis optica: Pathogenicity of patient immunoglobulin in vivo. *Ann Neurol.* 2009;66:630–643.
59. Lucchinetti CF, Mandler RN, McGavern D, et al. A role for humoral mechanisms in the pathogenesis of Devic's neuromyelitis optica. *Brain.* 2002;125(Pt 7):1450–1461.
60. Saadoun S, Waters P, Owens GP, Bennett JL, Vincent A, Papadopoulos MC. Neuromyelitis optica MOG-IgG causes reversible lesions in mouse brain. *Acta Neuropathol Commun.* 2014;2(1):35.

61. Dale RC, Tantsis EM, Merheb V, et al. Antibodies to MOG have a demyelination phenotype and affect oligodendrocyte cytoskeleton. *Neurol Neuroimmunol Neuroinflamm*. 2014;1(1):e12.
62. Ludwig RJ, Vanhoorelbeke K, Leypoldt F, et al. Mechanisms of autoantibody-induced pathology. *Front Immunol*. 2017;8:603.
63. Fossati-Jimack L, Reiningner L, Chicheportiche Y, et al. High pathogenic potential of low-affinity autoantibodies in experimental autoimmune hemolytic anemia. *J Exp Med*. 1999;190(11):1689–1696.
64. Flach AC, Litke T, Strauss J, et al. Autoantibody-boosted T-cell reactivation in the target organ triggers manifestation of autoimmune CNS disease. *Proc Natl Acad Sci U S A*. 2016;113(12):3323–3328.
65. Kinzel S, Lehmann-Horn K, Torke S, et al. Myelin-reactive antibodies initiate T cell-mediated CNS autoimmune disease by opsonization of endogenous antigen. *Acta Neuropathol*. 2016;132(1):43–58.